Journal of Engineering Research and Reports

16(1): 29-39, 2020; Article no.JERR.59966
ISSN: 2582-2926

Microstructural Characterization of Particulate Matter from Gasoline-Fuelled Vehicle Emissions

Bekir Güney[1*] and Ali Aladağ[2]

[1]Karamanoglu Mehmetbey University, Vocational School of Technical Sciences, 70200, Karaman, Turkey.
[2]Karamanoglu Mehmetbey University, Graduate School of Natural and Applied, Karaman, Turkey.

Authors' contributions

This work was carried out in collaboration between both authors. Author BG designed the study, performed the statistical analysis, wrote the protocol and wrote the first draft of the manuscript. Authors AA and BG managed the analyses of the study. Authors AA and BG managed the literature searches. Both authors read and approved the final manuscript.

Article Information

DOI: 10.9734/JERR/2020/v16i117157
Editor(s):
(1) Dr. Ravi Kant, Maharaja Ranjit Singh Punjab Technical University, India.
Reviewers:
(1) Raheel Jawad, India.
(2) Joaci Dos Santos Cerqueiranatural, Federal University of Campina Grande, Brazil.
Complete Peer review History: http://www.sdiarticle4.com/review-history/59966

Original Research Article

Received 23 July 2020
Accepted 12 August 2020
Published 20 August 2020

ABSTRACT

Exhaust emissions from vehicle traffic refers to the particles released into the air due to combustion of fuels, additives and wear of engine parts in the system during vehicle use. These emissions occur depending on the type of vehicle, type of fuel, combustion process and environmental conditions. In this study, microstructure and chemical characterization of particulate matter (PM) released from gasoline-fuelled vehicles were examined using electron microscopy techniques. As a result, much solid soot, metalloids, heavy metals, ash, sulphates, phosphates, minerals, volatile organic and inorganic pollutants were found to be present in gasoline exhaust emission. These toxic structures still pose a danger to environmental safety and human health.

Aim: In study, microstructure characterization of emissions released from gasoline-fuelled vehicles exhaust were investigated using electron microscopy techniques. Study design: SEM, EDS, XRD and FTIR electron microscopy techniques were used for characterization.

Place and Duration of Study: Material Characterization Laboratory of Karamanoğlu Mehmetbey University, Scientific and Technological Research Application and Research Center, between Junuary 2020 and July 2020.

**Corresponding author: Email: guneyb@kmu.edu.tr, guneyb03@hotmail.com;*

Results: The vehicles still continue to spread toxic pollutants.
Conclusions: The chemical structure of PM contains 20 elements including C, F, N, Na, O, Mg, Br, Si, Hg, S, P, Pb, Ca, Cr, Mn, Fe, Ni, Co, Cu, Zn. There are pollutant functional groups such as OH, CO, SO in the structure. Hydrocarbons, metalloids, heavy metals, different minerals, phosphates, sulfates, many volatile organic and inorganic compounds pollute the air in PM structure. These toxic pollutants harm the environment and human health.

Keywords: Emission; air pollution; microstructure; gasoline; SEM; FTIR; XRD; EDS.

1. INTRODUCTION

In recent years, atmospheric particulate matter pollution caused by rapid economic and social development has been significantly changing biodiversity. The negative effects of pollution on human health place the issue at the top of the international agenda. Air pollution has had many effects on the environment and human health [1], but its effects, especially on the cardiovascular system and other organs [2], increase the rates of disease and death [3].

Both natural resources (e.g. forest fires, volcanic eruptions, aerosolized soil and powders, pollen and moulds), as well as anthropogenic sources (e.g. industry, power plants, traffic, home heating, cooking, construction, mechanical wear, agriculture etc.) cause air pollution [4]. One of the most important sources is the exhaust emissions of motor vehicles using fossil fuels [5]. Gasoline vehicles, particulate matter (PM), carbon dioxide (CO_2), hydrocarbons (HC), nitrogen oxides (NO_x) and carbon monoxide (CO) [6], ammonia and volatile organic compounds (VOC) [5], semi-volatile liquid droplets, aldehydes, polycyclic aromatic hydrocarbons (PAHs), and metals [7] are the major sources of air pollution as combustion emissions. Among these, gaseous pollutants have short-and long-term health effects [8] due to their oxidative properties [9].

PM is one of the many by-products of spark-ignition engines (SI) [10], and is classified by particle size. Coarse particles (PM_{10}) are 10 µm or smaller in diameter, fine particles ($PM_{2.5}$) are 2.5 µm or smaller in diameter, and ultra-fine particles (or "nanoparticles") describe particles 100 nm or smaller in diameter [4]. A previous study reported that the size distribution and total exposure to particulates caused chronic and fatal health problems [11]. Besides, asbestos, carbon nanotubes or fullerenes in different forms of exhaust emission may accumulate in the lungs and exhibit similar dangerous effects [12].

PM or soot usually occurs in the combustion chamber in a rich fuel mixture [13]. In gasoline direct injection (GDI) engines, more soot is released due to lack of fuel evaporation and gas-phase mixing. Therefore, these engines are an important source of carbonaceous nanoparticles [14]. Soot production continues even if a homogeneous combustion process is achieved using different fuel injections [15]. Liquid fuel residue deposits on cylinder/piston walls [16], and the direct carbonization process of the remaining droplets are other important mechanisms of soot formation [17]. Nuclei with a diameter of 1 nm in the first phase of nucleation are generally characterized as primary particles [18]. A large part of the particulate matter, called secondary particles from the exhaust gas, occurs during this process of nucleation and solidification. This process of condensation and agglomeration also affects the composition, size and quantity of PM [19]. Due to the high atmospheric oxidation occurring in the process, the composite structure morphology consists of highly oxidized form [20]. The process occurs in both pre-mixed and non-pre-mixed combustion under Rich fuel conditions. The nucleation process begins with gas-phase condensation reactions at high temperatures between 726 and 2526 ^{0}C. In this process, unburned hydrocarbons, especially those in acetylene and polycyclic aromatic hydrocarbons (PAH), are pyrolyzed and oxidized. A large number of primary soot particles smaller than 2 nm in diameter are produced with this reaction. During the agglomeration process, nanoparticles grow by flaking. Although the number of particles decreases during this process, the total amount of particles remains constant. Amorphous aggregates (secondary particles) in the form of clusters or chains are formed by adhesion accumulation of hydrocarbon gas-phase species during the solidification process. In the final stage of soot formation, when appropriate conditions are provided, nuclei or aggregates are oxidized by interacting with oxidising forms such as O_2, O, OH, CO_2 and H_2O [18]. This formation is significantly affected by engine operating

conditions such as oxidation, injection modes [21], cooling conditions [22], engine speed and load [23] Besides, PM concentrations may include lubricating oil, engine part wear, fuel components, and compositions resulting from atmospheric conditions [24].

In similar studies in the relevant literature, various studies have been conducted on the impact of vehicle emissions on the environment [25-27], health [28,29] and characterization [30-34]. Microstructure analysis of vehicle emissions was performed in our previous studies [19,35,36]. Today, significant improvements have been made in terms of fuel efficiency and CO_2 emissions for gasoline engines due to the increasingly systematic introduction of emission control mechanisms [37]. However, while the issue of PM emissions has been extensively researched for diesel engines, very little research has been conducted on petrol engines. The difficulty in determining PM morphology may have been effective in this. In this study, microstructure and chemical characterization of PM emissions from gasoline-fuelled engines were examined. For this purpose, field scanning electron microscopy (SEM), energy dispersive spectrometer (EDS), X-ray diffraction (XRD) and Fourier Transform Infrared Spectroscopy (FTIR) were performed for PM collected from different cars operating under real atmospheric conditions.

2. MATERIALS AND METHODS

2.1 PM Collection

Vehicle-caused pollutant emissions are emitted into the environment under real-atmospheric conditions. Emission particles used in our study, were collected from 10 pieces passenger cars uses commercial LPG fuel in Karaman/Turkey. The cars were selected spark ignited, 4-cylinder, 2011-2020 model vehicles. Particle collection took place outside in the urban area from January 2020 to June 2020. Test vehicles were selected from well-maintained vehicles that traveled between 10000 km and 165000 km. The test vehicle emission particles under study, released by The Ministry of Turkey Environment and Urbanization" "*Regulation on Exhaust Gas Emission Control and Gasoline and Diesel Quality*" is collected on the basis of the specified limit values. The vehicles were operated at 750, 1750 and 2500 rpm fixed loads. Particle collection was carried out by accumulating on the glass surface placed at the end of the exhaust line in the cycles specified in the arrangement and in a stable regime (85-90 ^{0}C) at room temperature. The collected samples were stored in a glass bottle for laboratory tests. The collected particles were analyzed mixed as they emitted into the atmosphere.

2.2 Chemical Characterization

Although there are a large number of spark-ignited (SI) engines today, the number of studies on SI motor PM morphology is limited. This may be due to the acceptance that SI engines cause much less emissions compared to heavily emitted diesel engines. However, factors such as the lack of maintenance of the engines used, fuel quality and environmental conditions cause significant PM production. PM morphology is also determined using only electron microscopy, and this is both laborious and expensive. Motor vehicle PM is known to consist of solid soot, ash, metals, sulphates phosphates, minerals and semi-volatile organics. The species and characteristics of these pollutants need to be defined in detail. The morphology of PM emissions released from SI engines is more complex than soot powders and agglomerates released from classic engines. In gasoline-fuelled engines, at high combustion temperatures of 400-3000 ^{0}C, carbon nanotubes and other fullerene structures can be released. These engines, powered by fossil fuels, are potential carbon producers. Exposure of fuels to high temperatures in the open flame in the combustion mechanisms of vehicles can lead to the formation of nano-sized particles.

Microstructure analysis was performed in SEM (HITACHI SU5000) device equipped with EDS in Material Characterization Laboratory of Karamanoğlu Mehmetbey University, Scientific and Technological Research Application and Research Center. To understand brake wear crystal forms, a Bruker D8 enhanced diffractometer (λ = 1.5406 Å) with X-ray diffraction (XRD) Cu-Ka radiation was used. IR spectroscopy (Bruker Vertex 70 ATR) was used to measure the FTIR spectrum of the sample. The data were collected by vibration frequencies at 4000-400 cm^{-1}scanning range at 4 cm^{-1}spectral resolution.

3. RESULTS AND DISCUSSION

3.1 Characterization by SEM and EDS

SEM images have been analyzed in detail to identify the collected particles as they emerge into the atmosphere. Fig. 1 (a), the composition

of the PMS occurs during this time as a large part of the smoke released as a result of combustion is nucleated and solidified as a secondary particle with the 50 kX magnified micrograph. This process of condensation and agglomeration is consistent with XRD analysis in the form of fine particles, which generally produced oxide-crystalline and low amorphous PM. Agglomerates are composed of dense spherical and very complex compound particles based on charred motor oil. From the images, agglomerates, spherical (or oil droplet) particles, fibrous particles, volatile particles, and other categories of particles can be distinguished in sample morphology. It is also understood that water droplets belonging to O-H bonds exist in line with FTIR Spectra.

Regions 1, 2 of the micrograph 50.0 kX magnified given in Fig. 1 (a), and EDS peaks taken from point 3 are shown in Fig. 1(b), (c), and (d). The elemental analysis data for these peaks are given in Table 1. With the help of EDS analysis, it was found that the elemental composition of PM consists of 20 elements such as F, N, Na, Mg, Br, Si, Hg, S, P, PB, Ca, Cr, Mn, Fe, Ni, Co, Cu, Fr, Zn, in addition to carbon and oxygen.

The grey and white cloud-looking regions in the 30 kX magnified SEM micrograph of the gasoline PM shown in Fig. 2 (a) indicate the density of different forms of oxide structures. The peaks of the EDS spectrum taken from the surface of the micrograph is given in Fig. 2 (b). The elemental composition of the EDS analysis is again given in Table 1. The data in Table 1 shows atomically that C exists in quantities of > 40% and quantities of > 20% O. In light of this data, it is assumed that the oxidized structures in the PM structure are dense. Besides, the presence of CA > 7% atomically is linked to the source of fossil fuel. Nitrogen in the structure formed the source of NO_x formation. Again, the presence of elements such as S, Pb, Hg indicates that the toxic structures are dense.

It is evident from micrographs in Fig. 2 (a) 30 kX magnified, (c) 100 kX magnified and (d) 200 kX magnified that the microstructure of the gasoline emission PM is formed by clumping in the agglomeration process and contains mainly spherical particles. XRD analyses have also confirmed that the grey and white images within the structure constitute oxidized structures. The average grain size of the morphological structure is 50 nanometers (nm), $PM_{2,5}$ class is explained by the scale of the micrograph in Fig. 2 (c). The width of the XRD diffraction peaks should also be noted. This indicates the presence of small crystallites within the gasoline PM concentration of different oxides and other pollutants. SEM images and EDS data also support this view.

3.2 Characterization by XRD

Because of the solidification mechanism and agglomeration processes, the composition of PM belonging to gasoline fuels contains different structures. XRD analyses reveal that the smoke particles are largely crystalline in line with SEM micrographs. The presence of many elements in the chemical structure of PM has been found with the EDS analysis. This leads to the formation of numerous crystal forms in the structure of PM (Fig. 3). The way of identification of very complex emission PM with XRD and FTIR analyses was preferred in the study. In this study, main bond structures belonging to functional groups such as HC, CO, SO and NO were identified based on EDS analyses in Table 1. Methane (CH_4) obtained with XRD analyses has much higher global warming potential than CO_2 released directly into the actual atmosphere [38].

The CH_4 emissions seen in high methane number fuels may be due to ignition ejection from the engine into the atmosphere without combustion, as they are less reactive than higher chain hydrocarbons [39]. Besides, N_2O, N_2O_5, N_2O_4 crystals are present in the structure despite the low nitrogen oxide production potential of gasoline vehicles.

These structures are the sources of greenhouse gases similar to CO_2 [38]. The presence of ammonium (NH_4) emissions could have been caused by air/fuel mixture ratios. Hydrocarbon derivatives in different crystal systems and morphologies given extensively in Table 2 such as C_8H_8, C_2H_4, C_2H_6, $C_{16}H_{18}$ are predominantly within the PM of gasoline fuels. The high temperatures caused by combustion in engines may have triggered the high-intensity formation of HC emissions. Depending on the composition of gasoline fuels, leaded (PbO and its derivatives) and sulphurous (SO and its derivatives) compounds are present in the chemical structure of PM. Different crystalline minerals and compounds such as $Ca_3(Si_2O_4N_2)$ and $Fe_4(PO_4)_2O$, $Ca(CO)_3$, SiO_2 were identified withthe results of the analysis (Table 2) depending on the fuel source.

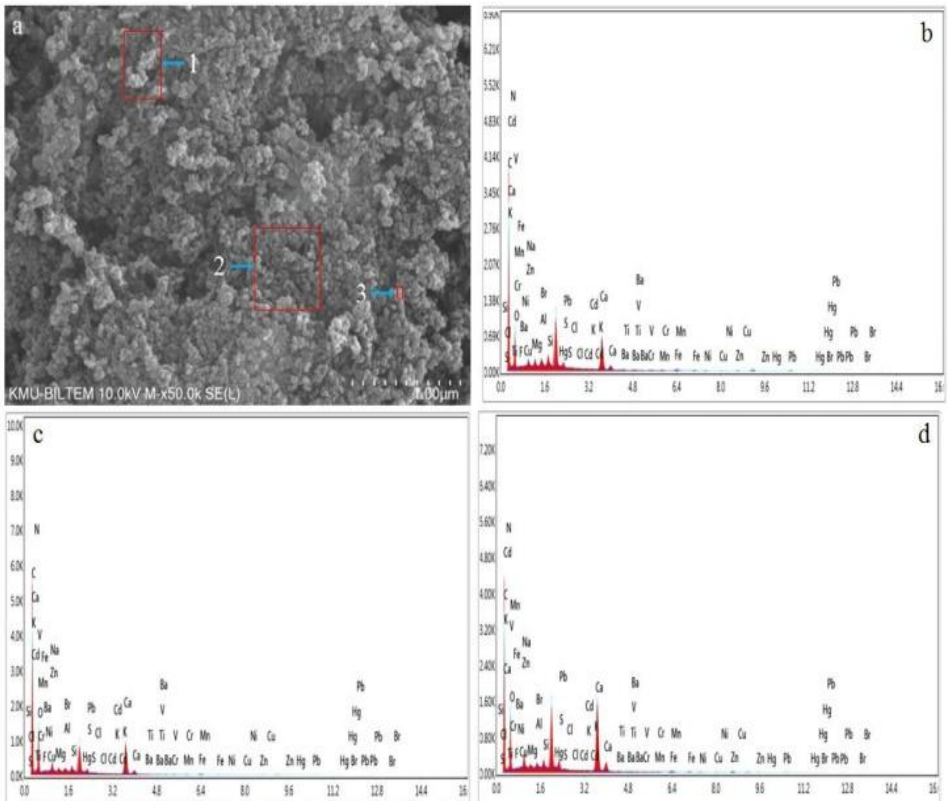

Fig. 1. SEM image and EDS spectra of petrol pm; a) 50.0 kX magnified image, b) EDS spectrum of Region 1 in (a), c) EDS spectrum of Region 2 in (a), d) EDS spectrum of Point 3 in (a)

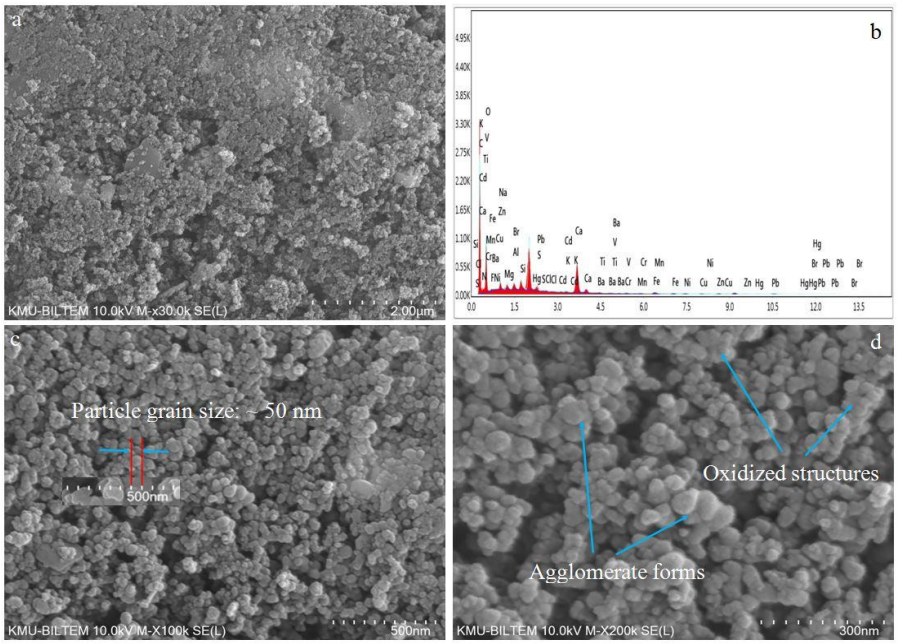

Fig. 2. SEM image and EDS spectra of petrol PM; a) 30.0 kX magnified image, b) EDS spectrum taken from the surface of the image in (a), c) 100 kX magnified image, d) 200 kX magnified image

Table 1. Atomic ratios of EDS analysis of elements of gasoline PM emissions

Element	Fig. 1(a)			Fig. 2(a)
	1. area	2. area	3.point	section
	Atomic %	Atomic %	Atomic %	Atomic %
C	40,58	46,19	56,82	49,21
F	4,67	3,02	1,78	1,36
N	2,67	2,76	7,78	5,36
Na	0,37		0,25	
O	34,41	25,98	20,75	28,23
Mg	0,67	1,38	0,99	0,96
Br	0,33	0,72	0,42	0,53
Si		2,07	1,04	1,12
Hg	0,32	0,54	0,25	0,23
S	0,12		0,18	0,21
P	0,32	0,14		
Pb	0,11	0,28		0,53
Ca	10,26	14,34	7,22	7,29
Cr	0,33			0,48
Mn	0,34		0,32	0,36
Fe	0,87	0,92	0,65	0,85
Ni	0,11			0,52
Co	0,22		0,43	0,12
Cu	0,26	0,45		0,57
Zn	1,69	0,85	0,93	1,29

Table 2. XRD spectra of particulate matter from gasoline fuel

Name	Formula	Crystal system	Peak Number
Calcium Nitride Silicate	$Ca_3(Si_2O_4N_2)$	Cubic	4,5,6,11
Picolinicacid N-oxide	$C_6H_5NO_3$	Monoclinic	4
Fukalite	$Ca_4(Si_2O_6)(CO_3)(OH)_2$	Orthorhombic	3,4,5,11,12
Cromium Ammine Nitrate	$Cr(NH_3)_6\ (NO_3)_3$		1,2,3,5
Tetrairon Oxide	$Fe_4(PO_4)_2\ O$	Monoclinic	1,5,6,7
Coesite	SiO_2	Monoclinic	3, 4, 6
Calcium Nitride Cyanide	$Ca(N(CN)_2)_2$	Monoclinic	1,2,3,4,6,7
Silicon Oxide	SiO_2	Cubic	2,4
Zinc Lead Oxide	$ZnPbO_3$		1,2,3,4,5,6,7,9,11,12
Zinc Iron Phosphate Hydrate	$Zn_4Fe_5(PO_4)_6\ (H_2O)_4$	Triclinic	1,2,3,4,5,6,7
Zinc Phosphide	ZnP_2	Orthorhombic	1,2,3,4,5,6,7
Mercury Phosphate	$(Hg_2)_3\ (PO_4)_2$	Monoclinic	1,2,3,4,5,6,7,9,10
Hydrogen Oxalate Hydrate	$(COOH)_{2\ 2H2O}$	Monoclinic	1,2,3,4,5,6,7
Thiourea	$SC(NH_2)_2$	Orthorhombic	1,2,3,4,
Sulfiric acid dihydrate	$(H_3O)_2SO_4$	Monoclinic	6
Sulfur Oxide	SO_3	Orthorhombic	1
Sulfur Oxide	S_8O	Orthorhombic	1,2,3,5,6,7,8,9
Calcium Lead Oxide	$Ca\ Pb\ O_{3-x}$	Cubic	4,6,12
Calcite	$Ca(CO)_3$	Rhombohedra	1,2,3,5,6,7
Calcium	Ca	Cubic	4,6,10
Litharge	PbO	Tetragonal	6,7,9,11,12
Lead Oxide	Pb_2O	Cubic	6,10

Name	Formula	Crystal system	Peak Number
Scrutinyite, syn	PbO_2	Orthorhombic	6,8,9,10
Minium, syn	Pb_3O_4	Tetragonal	4,6,7,8
Phosphorus Nitride	PbN_5	Orthorhombic	1,2,3,4
Lead Hydrate Acedate Oxide	$Pb(C_2H_3O_2)_2$ $Pb(OH)_2$ H_2O		1,2,3,4,5,6,7,8,9
Ammonium Hydrogen Phospahate	NH_4 H $(PO_3)_2$	Triclinic	3,4
Ammonium Zinc Nitrate Hydroxide Hydrate	NH_4 $Zn_5(OH)_9(NO_3)_2$ $3H_2O$		1,2,3,5,6,7
Carbondioxide	CO_2	Cubic	3,6,7
Paraffin wax	$(CH_2)_x$		2,3,7,12
Ethene	C_2H_4		1,2,3,4,6,8,9,12
Ethane	C_2H_6	Orthorhombic	1,2,3,7
α-Poly-p-xylylene	$(C_8H_8)_n$	Monoclinic	1,2,3,4
Docosane	$C_{22}H_{46}$	Triclinic	1,2,3
n-Heneicosane	$C_{21}H_{44}$	Orthorhombic	1,2
N-Hentriacontane	$C_{31}H_{64}$	Orthorhombic	1,2
Sexiphenyl	$C_{36}H_{26}$		1,2,3
n-Triacontane	$C_{30}H_{62}$	Monoclinic	1,2,3
Tolan	$C_{14}H_{10}$	Monoclinic	1,2,3
1,2 di-p-tolylethane	$C_{16}H_{18}$	Monoclinic	1,2,3
N-Hexacosane	$C_{26}H_{54}$	Triclinic	1,2,3
n-Tetracosane	$C_{24}H_{50}$	Triclinic	1,2,3
n-Nonacosane	$C_{29}H_{60}$	Orthorhombic	2
n-Octadecane	$C_{18}H_{38}$	Triclinic	1,3
Carpethite	$C_{24}H_{12}$	Monoclinic	1,3
Acenaphthene	$C_{12}H_{10}$	Orthorhombic	1,2,3,4
β-Fumaric acid	$C_4H_4O_4$	Triclinic	1,2,3,4
Dimethyl 2-acetyl-3-phenylsuccinate	$C_{14}H_{16}O_5$	Monoclinic	1,2,3,4
2-amino 4-methylpentanoic acid	$C_6H_{13}N_2O$	Triclinic	1,2,3,4,5
5-Methoxy-9 methylphenazine 5-oxide	$C_{14}H_{12}N_2O$		1,2,3,4
Guanidinium hydrogen L-aspartate	$C_5H_{12}N_4O_4$	Orthorhombic	1,2,3,4,5,6,7
5-Nitro uracil	$C_4H_3N_3O_4$		1,2,3,4,5,6,7
Ethyl nitrophenylthio triazole	$C_4H_{10}N_4O_2S$	Monoclinic	1,2,3,4,5
Dihydroxy-mercaptopyrimicline	$C_4H_4N_2O_2S$		1,2,3,4,5
Ammonium 1-aminoethane-1 1 diphosphonate dihydrate	$C_2H1_2N_2O_6P_2$ $2H_2O$	Orthorhombic	3,4,5,6,7
Iron Hydrogen Squarate Tetrahyrate	$C_8H_2FeO_8$ $4H_2O$	Triclinic	1,2,3,4
Hydrogen Oxalate Hydrate	$C_2H_2O_4$ $2H_2O$	Monoclinic	1,3,4,7
Tetrahydroxy-benzoquinone Dihydrate	$C_6H_4O_6$ $2H_2O$	Monoclinic	3,4,7
Guanine hydrochloride hydrate	$C_5H_5N_5O$ HCl H_2O	Monoclinic	1,3,4
Nitogen Oxide	N_2O	Orthorhombic	6, 7,8,11,12
Nitogen Oxide	N_2O_4	Orthorhombic	2,4,7,9,10,11
Nitogen Oxide	N_2O_5	Monoclinic	4, 10

3.3 Characterization by FTIR

The FTIR characterization of functional groups and other substances in the structure of PM was analysed between wavelengths of 400-4000 cm^{-1}. When many elements coexist, PM is a combination of many elements. However, FTIR spectroscopy is an appropriate method for the analysis of different combinations. With FTIR spectra, it is possible to determine the wide range of bond structures. However, PM is quite difficult to identify due to its scattering to the mid-infra-red spectrum and the very different absorption peaks that match with the condensed phase spectrum. However, thanks to the established standards, the determination of inorganic substances or organic functional groups has become easier. In this way, the bond structures of the elements in the PM structure were found to be in line with the EDS results. According to the peak values shown in Figure 4, OH molecules have shown their presence by producing large signals in the 2133-3928 cm^{-1} spectrum region.

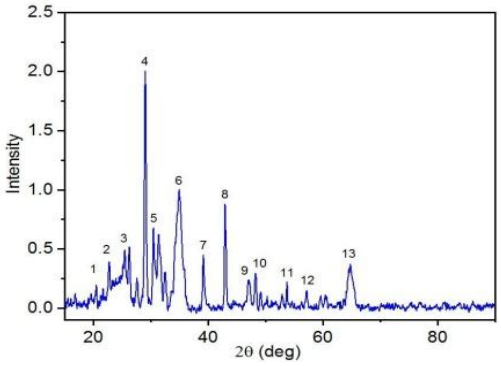

Fig. 3. XRD pattern of particulate matter derived from gasoline fuel

The peaks in the range of 1452-2919 cm^{-1} belonging to O-C stresses, which are carbonaceous bond structures, indicate the presence of CO_2 molecules in the structure. The peaks between 1554-2352 cm^{-1} indicate the presence of CO molecules. The peaks between 408-2352 cm^{-1} belonging to H-C stresses indicate the presence of HC molecules. At the moment of combustion in engines, temperatures rise to around 2000 ^0C. Thanks to this high energy, the exhaust temperature exceeds 1000 ^0C. It has also been confirmed by XRD models that hydrocarbon (HC) emissions occur at these temperatures. The peaks of 711-1554 cm^{-1} belonging to the S-O stresses indicate the presence of SO_2 molecule in the structure. The peaks in the 602-1018 cm^{-1} range of N-O stresses indicate that NO_x free and mixed bond molecules exist in the structure. As oxide structures undergo scattering below 1000 cm^{-1} [40], it is possible to mention the presence of oxide bonds in various forms in the 408-1018 cm^{-1} band range. Essentially, combustion products contain highly oxidized structures. EDS analysis and XRD Spectra also confirm this result.

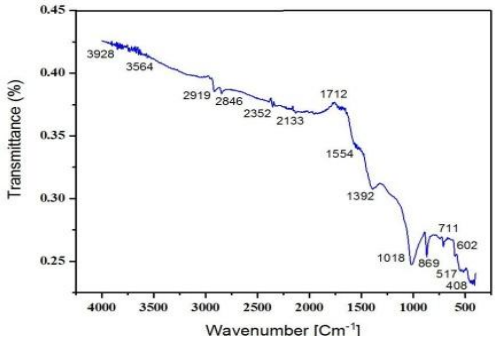

Fig. 4. FTIR spectra of particulate matter from gasoline fuel

In general, the fuel composition of gasoline may differ significantly according to the source. The chemical structure of PM may vary depending on fuel, vehicle, environment and combustion conditions. One of the main sources of PM in gasoline-fuelled engines is the inclusion of lubricating oil in the combustion process [41]. Furthermore, the additives in oil become volatile in the combustion process. The particle size distribution of these combinations was measured at an average of 50 nm according to the SEM micrograph in Fig. 2(c). This explains that particulate matter is included in the class $PM_{2.5}$. Ultra-thin grain-sized PM's being highly breathable increases respiratory system diseases [42]. Besides, these particles have a very harmful effect on humans, microorganisms, plants, animals, and the environment [43]. It is possible to predict that evaporating exhaust fumes and volatile substances increase the formation of nanoparticles due to the mechanism of inorganic nucleation and solidification. The EDS analysis points out that gasoline exhaust emissions are the source of many metalloids, heavy metals [44], and organic pollutants [45]. These substances are mostly bio toxic [46]. Metals are essential elements in biological translation. However, lack or excess of it emerges as environmental problems in underground and above-ground resources such as air, soil and water. The inability to dispose of heavy metals from the body is considered to be the cause of diseases. Occupational diseases in humans are the most important example of this.

As a result, gasoline fuels are a source of less NO_x emissions than diesel fuels, but they are an important source of environmental problems by emitting hydrocarbon emissions in more diverse formations.

4. CONCLUSION AND RECOMMENDATIONS

The study was conducted for the investigation of the microstructure and chemical characterization of PM released as a result of the burning of gasoline, which has been widely used over the last hundred years. SEM analyses reveal that PM occurs by solidification and agglomeration in ultra-thin nano-sizes, often in a crystalline and amorphous structure. With EDS analysis, the chemical structure of PM was found to contain 20 elements, C, F, N, Na, O, Mg, Br, Si, Hg, S, P, Pb, Ca, Cr, Mn, Fe, Ni, Co, Cu, Zn. With FTIR Spectra, low levels of NO_x emissions were found to exist. It has been found that HC emissions, which are mainly produced extensively by gasoline fuels, are present in different forms. Other functional groups such as OH, CO, SO were explained in the structure. XRD analyses revealed that hydrocarbons, metalloids, heavy metals, different minerals, phosphates, sulphates, and a large number of volatile organic and inorganic compounds were present in the structure in line with EDS and FTIR spectra. It has been found that emission of a very complex structure, which occurs due to engine type, fuel type, combustion process and environmental conditions, pollutes the environment. Although it produces very low levels of emissions compared to diesel fuels, it remains one of the major sources of environmental pollution in gasoline fuels. It should be noted that emissions cause significant damage to the environment due to their toxic properties. This is why the study is thought to offer useful information for policymakers and researchers.

ACKNOWLEDGEMENTS

This study was prepared by using the master thesis entitled "Microstructural characterization of particulate matter from vehicle emissions", supported by the 16-YL-19 Project accepted by the Scientific Research Projects Commission of Karamanoğlu Mehmetbey University. We would like to thank Karamanoğlu Mehmetbey University for its financial support.

COMPETING INTERESTS

Authors have declared that no competing interests exist.

REFERENCES

1. Schraufnagel DE, Balmes JR, Cowl CT, De Matteis S, Jung SH, Mortimer K, Thurston GD, et al. Air pollution and noncommunicable diseases: A review by the Forum of International Respiratory Societies' Environmental Committee, Part 2: Air pollution and organ systems. Chest. 2019;155(2):417-426.
2. Raftis JB, and Miller MR. Nanoparticle translocation and multi-organ toxicity: A particularly small problem. Nano Today. 2019;26:8-12.
3. Lelieveld J, Klingmüller K, Pozzer A, Pöschl U, Fnais M, Daiber A, Münzel T. Cardiovascular disease burden from ambient air pollution in Europe reassessed using novel hazard ratio functions. European Heart Journal. 2019;40(20): 1590-1596.
4. Miller MR. Oxidative stress and the cardiovascular effects of air pollution. Free Radical Biology and Medicine. 2020;151: 69-87.
5. de Miranda RM, de Fatima Andrade M, Fornaro A, Astolfo R, de Andre PA, and Saldiva P. Urban air pollution: A representative survey of PM 2.5 mass concentrations in six Brazilian cities. Air Quality Atmosphere & Health. 2012;5(1): 63-77.
6. Watany M. Variability in vehicle'exhaust emissions and fuel consumption in urban driving pattern. American Journal of Vehicle Design. 2015;3(1):31-38.
7. Reşitoğlu İA, Altinişik K, and Keskin A. The pollutant emissions from diesel-engine vehicles and exhaust aftertreatment systems. Clean Technologies and Environmental Policy. 2015;17(1):15-27.
8. Brook RD, Rajagopalan S, Pope III CA, Brook JR, Bhatnagar A, Diez-Roux A, Peters, A. by et al. Particulate matter air pollution and cardiovascular disease: An update to the scientific statement from the American Heart Association. Circulation. 2010;121(21):2331-2378.
9. Auerbach A, Hernandez ML. The effect of environmental oxidative stress on airway inflammation. Current Opinion in Allergy and Clinical Immunology. 2012; 12(2):133.
10. Englert N. Fine particles and human health-a review of epidemiological studies. Toxicology letters. 2004;149(1-3):235-242.

11. Oberdörster G, Oberdörster E, Oberdörster J. Nanotoxicology: An emerging discipline evolving from studies of ultrafine particles. Environmental Health Perspectives. 2005; 113(7):823-839.
12. Donaldson K, Murphy FA, Duffin R, Poland CA. Asbestos, carbon nanotubes and the pleural mesothelium: A review of the hypothesis regarding the role of long fibre retention in the parietal pleura, inflammation and mesothelioma. Particle and Fibre Toxicology. 2010;7(1):5.
13. Bockhorn HA. Short introduction to the problem-Structure of the following parts. In Soot Formation in Combustion. Springer, Berlin, Heidelberg. 1994;3-7.
14. Piock W, Hoffmann G, Berndorfer A, Salemi P, Fusshoeller B. Strategies towards meeting future particulate matter emission requirements in homogeneous gasoline direct injection engines. SAE International Journal of Engines. 2011; 4(1): 1455-1468.
15. Williams B, Ewart P, Wang X, Stone R, Ma H, Walmsley H, Wallace S, et al. Quantitative planar laser-induced fluorescence imaging of multi-component fuel/air mixing in a firing gasoline-direct-injection engine: Effects of residual exhaust gas on quantitative PLIF. Combustion and Flame. 2010;157(10):1866-1878.
16. Lucchini T, Errico GD, Onorati A, Bonandrini G, Venturoli L, Gioia RD. Development and application of a computational fluid dynamics methodology to predict fuel–air mixing and sources of soot formation in gasoline direct injection engines. International Journal of Engine Research. 2014;15(5):581-596.
17. Maricq M, Podsiadlik D, Brehob D, Haghgooie M. Particulate emissions from a direct-injection spark-ignition (DISI) engine. SAE Technical Paper. 1999;1-1530.
18. La Rocca A, Bonatesta F, Fay MW, Campanella F. Characterisation of soot in oil from a gasoline direct injection engine using Transmission Electron Microscopy. Tribology International. 2015;86:77-84.
19. Güney B, Öz A. Microstructure and chemical analysis of NOx and particle emissions of diesel engines. International Journal of Automotive Engineering and Technologies. 2020;9(2):105-112.
20. Clague ADH, Donnet JB, Wang TK, Peng JCM. A comparison of diesel engine soot with carbon black. Carbon. 1999;37(10): 1553-1565.
21. Li X, Guan C, Luo Y, Huang Z. Effect of multiple-injection strategies on diesel engine exhaust particle size and nanostructure. Journal of Aerosol Science. 2015;89:69-76.
22. Wang Q, Yao C, Dou Z, Wang B, Wu T. Effect of intake pre-heating and injection timing on combustion and emission characteristics of a methanol fumigated diesel engine at part load. Fuel. 2015;159: 796-802.
23. Saffaripour M, Chan TW, Liu F, Thomson K A, Smallwood GJ, Kubsh J, Brezny R. Effect of drive cycle and gasoline particulate filter on the size and morphology of soot particles emitted from a gasoline-direct-injection vehicle. Environmental Science & Technology. 2015;49(19):11950-11958.
24. Pfau SA, La Rocca A, Haffner-Staton E, Rance GA, Fay MW, Brough RJ, Malizia S. Comparative nanostructure analysis of gasoline turbocharged direct injection and diesel soot-in-oil with carbon black. Carbon. 2018;139:342-352.
25. Andres RJ, Boden TA, Bréon FM, Ciais P, Davis S, Erickson D, Gregg JS, Jacobson A, Marland G, Miller J, Oda T, Olivier JGJ, Raupach MR, Rayner P, Treanton K. A synthesis of carbon dioxide emissions from fossil-fuel combustion. Biogeosciences. 2012;9:1845-1871.
26. Andres RJ, Gregg JS, Losey L, Marland G, and Boden TA. Monthly, global emissions of carbon dioxide from fossil fuel consumption. Tellus B: Chemical and Physical Meteorology. 2011;63(3):309-327.
27. Platt SM, El Haddad I, Zardini AA, Clairotte M, Astorga C, Wolf R, Drinovec L. Močnik G, Möhler O, Richter R, Barmet R, Bianchi F, Baltensperger U, Prévôt ASH. Secondary organic aerosol formation from gasoline vehicle emissions in a new mobile environmental reaction chamber. Atmospheric Chemistry Physics. 2013;13: 9141-9158.
28. Liang X, Zhang S, Wu X, Guo X, Han L, Liu H, Wu Y, Hao J. Air quality and health impacts from using ethanol blended gasoline fuels in China. Atmospheric Environment. 2020;228:117396.
29. Neyestani SE, Walters S, Pfister G, Kooperman GJ, Saleh R. Direct radiative effect and public health implications of aerosol emissions associated with shifting to Gasoline Direct Injection (GDI) technologies in light-duty vehicles in the

United States. Environmental Science & Technology. 2019;54(2):687-696.
30. Yang HH, Dhital NB, Wang LC, Hsieh YS, Lee KT, Hsu YT, and Huang SC. Chemical characterization of fine particulate matter in gasoline and diesel vehicle exhaust. Aerosol and Air Quality Research. 2019; 19(6):1349-1449.
31. Lin YC, Li YC, Amesho KT, Shangdiar S, Chou FC, and Cheng PC. Chemical characterization of PM2. 5 emissions and atmospheric metallic element concentrations in PM2. 5 emitted from mobile source gasoline-fueled vehicles. Science of The Total Environment. 2020; 739:139942.
32. Ağbulut Ü, Ayyıldız M, Sarıdemir S. Prediction of performance, combustion and emission characteristics for a dual fuel diesel engine at varying injection pressures. Energy. 2020;117257.
33. Ağbulut Ü, Sarıdemir S, and Albayrak S. Experimental investigation of combustion, performance and emission characteristics of a diesel engine fuelled with diesel–biodiesel–alcohol blends. Journal of the Brazilian Society of Mechanical Sciences and Engineering. 2019;41(9):389.
34. Uyumaz A, Aksoy F, Mutlu İ, Akbulut F, Yılmaz E. The pyrolytic fuel production from nutshell-rice husk blends and determination of engine performance and exhaust emissions in a direct injection diesel engine. International Journal of Automotive Engineering and Technologies. 2018;7(4):134-141.
35. Güney B, and Küçüksarıyıldız H. Taşıt Emisyonlarının Mikroyapı Analizi. Afyon Kocatepe Üniversitesi Fen Ve Mühendislik Bilimleri Dergisi. 2019;19(3): 884-893.
36. Güney B, Öz A. Microstructure and chemical analysis of vehicle brake wear particle emissions. Avrupa Bilim ve Teknoloji Dergisi. 2020;19:633-642.
37. Zhao F, Lai MC, Harrington DL. Automotive spark-ignited direct-injection gasoline engines. Progress in energy and combustion science. 1999;25(5):437-562.
38. Karavalakis G, Hajbabaei M, Jiang Y, Yang J, Johnson KC., Cocker DR, Durbin TD. Regulated, greenhouse gas, and particulate emissions from lean-burn and stoichiometric natural gas heavy-duty vehicles on different fuel compositions. Fuel. 2016;175:146-156.
39. Burcat A, Scheller K, Lifshitz A. Shock-tube investigation of comparative ignition delay times for C1-C5 alkanes. Combustion and Flame. 1971;16(1):29-33.
40. Lagashetty A, Havanoor V, Basavaraja S, Balaji SD, and Venkataraman A. Microwave-assisted route for synthesis of nanosized metal oxides. Science and Technology of Advanced Materials. 2007;8(6), 484-493.
41. Wang WG, Clark NN, Lyons DW, Yang, RM, Gautam M, Bata RM, Loth JL. Emissions comparisons from alternative fuel buses and diesel buses with a chassis dynamometer testing facility. Environmental Science & Technology. 1997;31(11):3132-3137.
42. Brunekreef B, Holgate ST. Air pollution and healthi. The Lancet. 2002;360(9341): 1233-1242.
43. Tiwari J, Tarale P, Sivanesan S, and Bafana A. Environmental persistence, hazard, and mitigation challenges of nitroaromatic compounds. Environmental Science and Pollution Research. 2019;26: 28650-28667.
44. Faiz Y, Tufail M, Javed MT, Chaudhry MM. Road dust pollution of Cd, Cu, Ni, Pb and Zn along islamabad expressway, Pakistan. Microchemical Journal. 2009;92(2):186-192.
45. Arya R, Baral B, Vigneswaran S, Naidu R, Loganathan P. Seasonal influence on urban dust PAH profile and toxicity in Sydney, Australia. Water Science and Technology. 2011;63(10):2238-2243.
46. Gromaire-Mertz MC, Garnaud S, Gonzalez A, Chebbo G. Characterisation of urban runoff pollution in Paris. Water Science and Technology. 1999;39(2): 1-8.

Peer-review history:
The peer review history for this paper can be accessed here:
http://www.sdiarticle4.com/review-history/59966